Visible-light induced electron emission from carbon nanotube forests

Parham Yaghoobi, Mehran Vahdani Moghaddam, Mario Michan, and Alireza Nojeh[a)]
Department of Electrical and Computer Engineering, The University of British Columbia, Vancouver, British Columbia V6T 1Z4, Canada

(Received 25 August 2010; accepted 21 November 2010; published 11 January 2011)

The authors report electron emission from forests of vertically aligned multiwalled carbon nanotubes under irradiation by continuous wave green and blue lasers with relatively low power and intensity (maximum intensity of ~320 W cm^{-2}). The electron emission shows nonlinear increase with laser power for both laser wavelengths of 488 and 532 nm. Thermionic emission and photofield-emission appear to play a role in different sections of the current-voltage characteristics. © *2011 American Vacuum Society.* [DOI: 10.1116/1.3526573]

I. INTRODUCTION

Low-voltage operation, long lifetime, high stability, and high brightness are some of the attractive properties of carbon nanotube (CNT) electron sources.[1] Despite the significant amount of research carried out on nanotube electron sources since the mid-1990s, much remains to be explored. An overwhelming majority of the previous works have been concerned with field-emission,[2–4] and less effort has been devoted to other emission mechanisms such as thermionic emission. One of the earliest reports on thermionic emission from CNTs was that of Cox *et al.*, who resistively heated a single multiwalled carbon nanotube (MWNT).[5] Since CNTs are expected to have high thermal conductivity, they attributed their observation of thermionic emission to the defective nature of their MWNTs, which must have a poor thermal conductivity. Two subsequent works that reported thermionic emission consist of resistively heating single-walled, double-walled, and multiwalled CNT bundles[6] and CNT yarns,[7] and measuring their respective workfunctions. Wei *et al.* also used thermionic emission and studied the work function of CNT yarns and sheets.[8] Thermally assisted field-emission was also observed in a work by Wong *et al.*, who heated a film of randomly distributed MWNTs using pulsed lasers with wavelengths of 532 and 355 nm.[9] However, the laser intensities used in those experiments were several orders of magnitude higher than the intensities used in the present work. Westover *et al.* demonstrated that thermionic emission from potassium-intercalated CNTs can be enhanced by photoexcitation of electrons using laser illumination.[10]

Other works have investigated the effect of laser irradiation on CNTs. Bassil *et al.* examined the effect of laser heating on Raman spectra.[11] They observed more effective heating of CNTs at the 488 nm laser wavelength than at 647 nm. Nakamiya *et al.* investigated the damage threshold of MWNT films using pulsed lasers at the first two harmonics of a Nd:YAG laser (λ=1064 and 532 nm) and a pulsed KrF excimer laser (λ=248 nm).[12,13] They measured the minimum energies (and calculated the corresponding temperatures) that damage and graphitize MWNT films.

Here, we demonstrate the effect of laser power and wavelength on electron emission from vertically standing MWNT forests using continuous wave (CW) laser. At low electric fields (below field-emission), the dominant laser-induced electron emission mechanism appears to be thermionic emission. At higher fields, prior to current saturation, photofield-emission is observed. This type of laser-controlled electron source has great potential for various applications, ranging from electron beam lithography to electron beam machining and vacuum electronics.

II. METHODOLOGY

Millimeter long, vertically aligned MWNT forests were grown on a highly *p*-doped silicon substrate using ethylene-based chemical vapor deposition at 750 °C. As catalyst (unpatterned), 1 nm of iron was evaporated on a 10 nm layer of alumina using electron beam evaporation. Before growth, the substrate was cleaved into small pieces (~2×4 mm^2).

Chips with CNT forests were mounted on a specially made sample holder and placed in a high vacuum chamber (~10^{-7} Torr). The CNT forests were used as the cathode and a copper sheet was used as the anode, placed approximately 1 mm above the top surface of the CNT forests. The current was measured through the cathode. Laser light was brought into the chamber through a 200 μm diameter optical fiber and collimated on the sidewall of the forest (Fig. 1). The collimated beam covered an area of approximately 0.8 mm^2 of the side of the CNT forest. A Coherent Verdi V-5 laser (λ=532 nm) and the main mode of an argon ion laser (λ=488 nm) from a Spectra-Physics Beamlok 2060-10S equipped with electronics to stabilize the cavity for single mode operation (Z-lock and J-lock) were used as laser sources. A Keithley 6517A source/electrometer was used to apply voltage and measure the current.

III. RESULTS AND DISCUSSION

The current-voltage characteristics of the CNT forest at different laser powers are illustrated in Fig. 2. It is apparent that field-emission gradually becomes dominant at all power levels above 200 V (corresponding to an electric field of 0.2 V $μm^{-1}$) and the current saturates at about 300 V. There are three distinct regions (as labeled on Fig. 2). In region I,

a)Electronic mail: anojeh@ece.ubc.ca

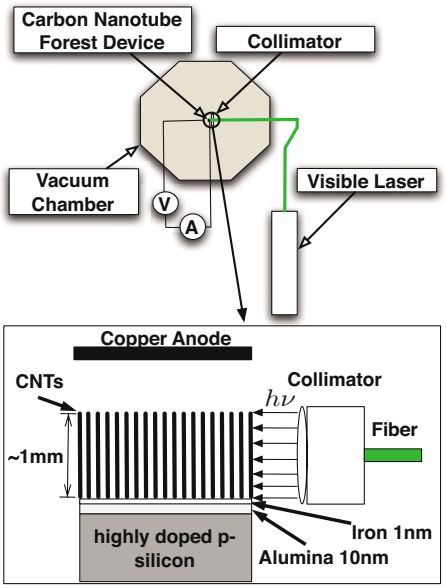

FIG. 1. (Color online) Schematic (not to scale) of the experimental configuration. The nanotube forest was grown on 1 nm of iron deposited on 10 nm of alumina. The laser irradiated the sidewall of the forest.

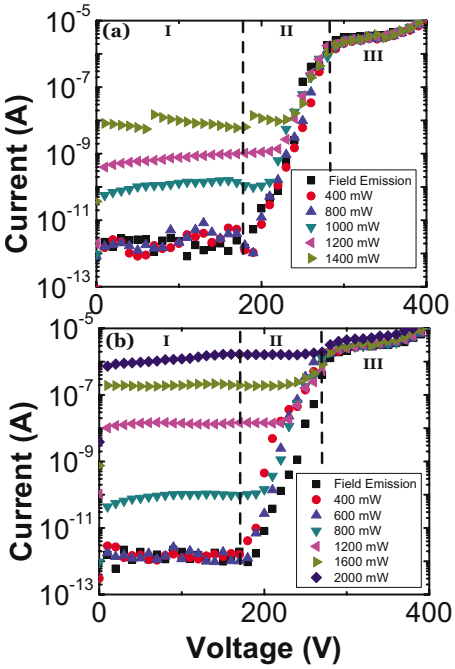

FIG. 2. (Color online) Emission current-voltage characteristics of the nanotube forest under different powers of (a) 488 nm laser (the kinks on the 1400 mW curve are due to the stabilization electronics of the high power single mode operation of the argon laser) and (b) 532 nm laser. There are three distinct regions in the current-voltage characteristics.

laser power has a drastic effect on the emission current. In region II, both the applied field and the laser play a role, and a transition takes place where the relative effect of the laser decreases as the strength of the applied field increases. In region III, the laser has little effect on the electron emission and field-emission seems to be the only significant emission mechanism. Our interest in this work thus lies in regions I and II, which will be discussed in detail in the remainder of this section.

There are three mechanisms that could explain electron emission due to laser irradiation at low electric fields (region I of Fig. 2), namely, photoemission, optical field-emission, and thermionic emission. Simple photoemission cannot be the case since the photon energies involved (2.3 and 2.54 eV) are not high enough to enable the electrons to overcome the nanotube work function barrier (4–5 eV). Also, for photoemission, one expects a linear increase of current as a function of laser power, as we previously demonstrated on CNT forests.[14] Figure 3 illustrates the emission current as a function of power at the wavelength of 532 nm. The emission current grows nonlinearly as a function of power. By the same argument, two photon-photoemission is also likely not the cause of the emission current behavior in region I in Fig. 2.

In order to fit the experimental data to optical field-emission, we have to consider the effective DC electric field of the laser due to its intensity. This can be estimated by approximating the laser's electromagnetic wave as a plane wave. The magnitude of the plane wave's time averaged Poynting vector is $\langle S\rangle=(\epsilon_0 c/2)E_0^2$, where ϵ_0 is the permittivity of free space, c is the speed of light, and E_0 is the electric field amplitude. Given the ~1 mm diameter of the laser beam spot that is irradiating the CNT forest, the effective electric field will be ~0.03 V μm^{-1} for a power level of 1 W. This field is about two orders of magnitude smaller than the needed field for field-electron emission from CNTs (which is ~1 V μm^{-1} before taking into account the field enhancement by the CNTs).

Thermionic emission may be modeled by Richardson's equation, $J=A_G T^2 e^{(-\Phi/kT)}$, where J is the current density, A_G is Richardson's constant, T is temperature, k is Boltzmann's constant, and Φ is the work function of the material. In order to examine whether thermionic emission can explain the observed behavior in region I, we need to estimate the temperature of the forest due to laser heating. This can be done by writing the power equilibrium equation for the system. The

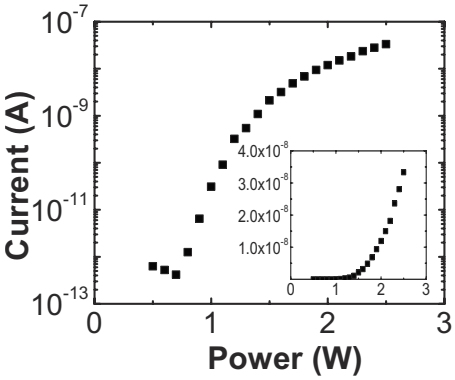

FIG. 3. Emission current as a function of the incident optical power for illumination by the 532 nm laser. Only 1 V of bias was applied for collection of electrons and there was no field-emission in this case. Inset shows the curve on linear scale.

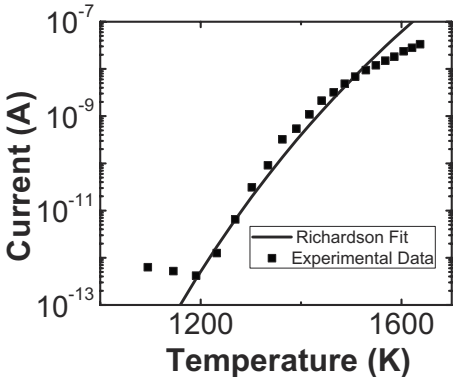

FIG. 4. Emission current as a function of the calculated temperature by the 532 nm laser. Only 1 V of bias was applied for collection of electrons and there was no field-emission in this case. The solid line shows the Richardson fit to the data.

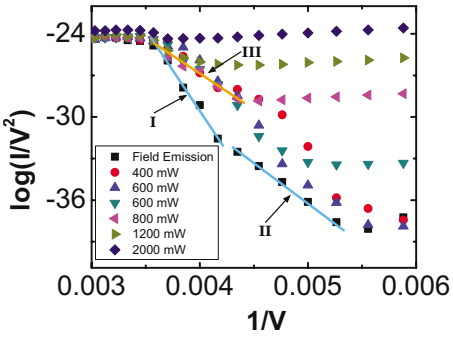

FIG. 5. (Color online) Fowler–Nordheim plot corresponding to the data in Fig. 2(b). Indicated are two different slopes on the (no laser) field-emission curve (slopes I and II) and a third slope (slope III) on the low-laser-power curve at high fields. The ratio of slopes I and III is ~2.9.

laser power input should dissipate in the system through emission of electrons and black body radiation. This can be expressed as[8]

$$P_{\text{laser}} = (\Phi + 2kT)A_G A T^2 e^{(-\Phi/kT)} + A\epsilon\sigma T^4, \quad (1)$$

where A is the area of the laser spot, σ is the Stefan–Boltzmann constant and ϵ is the emissivity of the material (which is close to 1 for dark materials such as CNTs). The first term on the right hand side of the equation is the power dissipated due to emission of electrons through a thermionic process (Richardson's law) and the second term is the power dissipated through black body radiation (Stefan–Boltzmann law). For simplicity, we have ignored the heat transfer to the substrate, since we do not have much information on the heat conduction at the CNT forest and substrate junction. This assumption has previously been observed to be correct in a similar situation.[8]

By using this expression, the temperature of the CNTs due to laser heating was calculated and then used in Richardson's equation, which shows a reasonable fit to our experimental data (Fig. 4). Note that in these experiments, we had no visual contact with the device inside the vacuum chamber in order to observe an incandescent glow as a result of the high temperature. In subsequent, related experiments, we have indeed observed such a glow, and the corresponding optical spectra indicate temperatures in the range of 1000–2000 K. The details of those experiments are beyond the scope of this article and will be reported in the future.

At high temperatures, the fit diverges from the data, which may be because our power measurements were done before the laser beam was coupled into the fiber. The beam waist of the laser increases (by a small amount) with increasing power, which is typically due to imperfections of the laser's cavity. This increase in waist size can reduce the amount of coupling between the laser and the fiber at high powers, which could provide an explanation for the observed behavior.

In region II of the current-voltage characteristics, both the applied field and the laser have an effect, and the relative effect of the laser decreases as the field increases. In this region, photofield-emission, that is the excitation of electrons to higher energy levels as a result of absorption of photons and their subsequent tunneling through the vacuum barrier, could play an important role. To understand this laser-assisted field-emission region better, we plot the data of Fig. 2(b) on the so-called Fowler–Nordheim (FN) scales[15,16] in Fig. 5. In region II, we can see two distinct slopes (slopes I and II) on the (no laser) field-emission curve (it should be noted that multiple linear regions on FN curves have been observed in CNT field emitters before). However, on the low-laser-power curves (400, 600, and 800 mW), there is a distinct third slope (slope III), which differs from the pure field-emission slope at similar fields. The ratio of slopes on FN axes is equal to the ratio of the effective work functions corresponding to the curves to the power of one-half [i.e., $(\Phi_1)^{1.5}/(\Phi_2)^{1.5}$]. In this case, the ratio of slope I to slope III is ~2.9. This value is very close to the ratio of the work function of a CNT (~4.6 eV) divided by the reduced work function of a CNT by photons with energy of 2.3 eV ($\lambda = 532$ nm) to the power of one-half [i.e., $(\Phi_{\text{CNT}})^{1.5}/(\Phi_{\text{CNT}} - E_{\text{photon}})^{1.5} = (4.6)^{1.5}/(2.3)^{1.5} \approx 2.8$]. It appears that when the electric field is high enough and the laser power is too low for thermionic emission (i.e., region II of the current-voltage curve at low laser power), photofield-emission can play an important role. If the optical power is further increased (the curves corresponding to 1200 and 2000 mW), the relative effect of the field becomes less pronounced and it becomes more difficult to observe this photofield-emission effect in the transition region II. Adsorbates also have an effect on the workfunction of a material and their desorbtion as a result of laser heating could alter the effective workfunction, thus affecting the emission current. However, their effect is usually less than 1 eV in terms of workfunction change.[17] Nonetheless, we cannot rule out the possibility that adsorbates may play a role in this emission regime, despite the high vacuum level of $\sim 10^{-7}$ Torr used in the experiments.

Light activated electron sources can have applications ranging from radio frequency cathodes used in accelerators and free-electron lasers to modern solar cells.[18] In this work, we have demonstrated thermionic electron emission from CNT forests with a light intensity that is several orders of

magnitude smaller than previously reported for CNT films (Ref. 9). This low-power-light activated electron source can not only improve the performance of electron sources in existing applications, but it can also enable new applications in microvacuum technology, such as on-chip electron sources activated using integrated lasers.

IV. SUMMARY

Millimetrer-long vertical MWNTs were irradiated with CW visible lasers with wavelengths of 532 and 488 nm. Three distinct regions of electron emission were identified. In the first region (at low electric fields), laser irradiation has a significant effect on the emission current, with strongly nonlinear increase in current as a function of laser power. The mechanism responsible for this behavior was identified as being primarily laser-induced thermionic emission. The second region of the current-voltage characteristics only shows a minor dependence on laser power and, at high electric fields in this region, photofield-emission is playing a role. The third region seems to be dominated by field-emission since all the curves saturate to almost the same level. The first two regions of emission due to laser can have applications in vacuum electronics and electron beam lithography and machining.

ACKNOWLEDGMENTS

The authors acknowledge financial support from the Natural Sciences and Engineering Research Council (NSERC Grant Nos. 341629-07 and 361503-09), the Canada Foundation for Innovation (CFI Grant No. 13271), the British Columbia Knowledge Development Fund (BCKDF), the BCFRST Foundation, and the British Columbia Innovation Council. P.Y. thanks the Department of Electrical and Computer Engineering, the University of British Columbia (UBC), and the Institute for Computing, Information, and Cognitive Systems (ICICS) at UBC for additional support. M.M. thanks the Bullitt Foundation for a graduate fellowship.

[1] N. de Jonge and J.-M. Bonard, Philos. Trans. R. Soc. London **362**, 2239 (2004).
[2] J.-M. Bonard, H. Kind, T. Stöckli, and L.-O. Nilsson, Solid-State Electron. **45**, 893 (2001).
[3] P. Yaghoobi and A. Nojeh, Mod. Phys. Lett. B **21**, 1807 (2007).
[4] N. de Jonge, Adv. Imaging Electron Phys. **156**, 203 (2009).
[5] D. C. Cox, R. D. Forrest, P. R. Smith, and S. R. P. Silva, Appl. Phys. Lett. **85**, 2065 (2004).
[6] P. Liu, Q. Sun, F. Zhu, K. Liu, K. Jiang, L. Liu, Q. Li, and S. Fan, Nano Lett. **8**, 647 (2008).
[7] P. Liu, Y. Wei, K. Jiang, Q. Sun, X. Zhang, S. Fan, S. Zhang, C. Ning, and J. Deng, Phys. Rev. B **73**, 235412 (2006).
[8] Y. Wei, K. Jiang, X. Feng, P. Liu, L. Liu, and S. Fan, Phys. Rev. B **76**, 045423 (2007).
[9] T.-H. Wong, M. C. Gupta, and C. Hernandez-Garcia, Nanotechnology **18**, 135705 (2007).
[10] T. L. Westover, A. D. Franklin, B. A. Cola, T. S. Fisher, and R. G. Reifenberger, J. Vac. Sci. Technol. B **28**, 423 (2010).
[11] A. Bassil, P. Puech, L. Tubery, W. Bacsa, and E. Flahaut, Appl. Phys. Lett. **88**, 173113 (2006).
[12] T. Nakamiya, T. Ueda, T. Ikegami, K. Ebihara, and R. Tsuda, Curr. Appl. Phys. **8**, 400 (2008).
[13] T. Nakamiya, T. Ueda, T. Ikegami, F. Mitsugi, K. Ebihara, Y. Sonoda, Y. Iwasaki, and R. Tsuda, Thin Solid Films **517**, 3854 (2009).
[14] P. Yaghoobi, M. Michan, and A. Nojeh, Appl. Phys. Lett. **97**, 153119 (2010).
[15] E. L. Murphy and R. H. Good, Jr., Phys. Rev. **102**, 1464 (1956).
[16] R. G. Forbes, J. Vac. Sci. Technol. B **17**, 526 (1999).
[17] C.-W. Chen and M.-H. Lee, Diamond Relat. Mater. **12**, 565 (2003).
[18] J. W. Schwede *et al.*, Nature Mater. **9**, 762 (2010).